Molecular Pharmacology Fast Forward. Published on April 6, 2017 as DOI: 10.1124/mol.117.108233
This article has not been copyedited and formatted. The final version may differ from this version.



**TITLE PAGE**

# *In vivo* characterization of an AHR-dependent long non-coding RNA required for proper *sox9b* expression

**Gloria R. Garcia, Britton C. Goodale, Michelle W. Wiley, Jane K. La Du, David A. Hendrix, Robert L. Tanguay**

Department of Environmental & Molecular Toxicology, Environmental Health Sciences Center, (G.R.R, J.K.L., R.L.T.), and Department of Biochemistry and Biophysics (M.W.W., D.A.H), Oregon State University, Corvallis, OR

Department of Microbiology and Immunology (B.C.G), Geisel School of Medicine at Dartmouth, Hanover, NH

Molecular Pharmacology Fast Forward. Published on April 6, 2017 as DOI: 10.1124/mol.117.108233
This article has not been copyedited and formatted. The final version may differ from this version.



**RUNNING TITLE PAGE**

Running title: AHR-dependent expression of *slincR* is required for reduction of *sox9b*

To whom correspondence should be addressed: Prof. Robert L. Tanguay, Department of Environmental & Molecular Toxicology, Sinnhuber Aquatic Research Laboratory Oregon State University, 28645 East Hwy 34, Corvallis, OR 97333, Telephone: (541) 737-6514; FAX: (541) 737-0497; Email: robert.tanguay@oregonstate.edu

Text pages: 39

Tables: 2 (1 is Supplemental)

Figures: 8 (2 are Supplemental)

References: 65

Abstract (words): 235

Introduction (words): 726

Discussion (words): 1246

The abbreviations used are: AHR, aryl hydrocarbon receptor; AHRE, aryl hydrocarbon responsive element; ARNT, aryl hydrocarbon nuclear translocator; B[*a*]AQ, benz(*a*)anthracene-7-12-dione; hpf, hour post fertilization; lncRNA, long non-coding RNA; slincR, sox9b long intergenic non-coding RNA; sox9, SRY-type box 9; TCDD, 2,3,7,8-tetrachlorodibenzo-*p*-dioxin.

Molecular Pharmacology Fast Forward. Published on April 6, 2017 as DOI: 10.1124/mol.117.108233
This article has not been copyedited and formatted. The final version may differ from this version.



**ABSTRACT**

Xenobiotic activation of the aryl hydrocarbon receptor (AHR) by 2,3,7,8-tetrachlorodibenzo-*p*-dioxin (TCDD) prevents the proper formation of craniofacial cartilage and the heart in developing zebrafish. Downstream molecular targets responsible for AHR-dependent adverse effects remain largely unknown; however, in zebrafish *sox9b* has been identified as one of the most reduced transcripts in several target organs and is hypothesized to have a causal role in TCDD-induced toxicity. The reduction of *sox9b* expression in TCDD-exposed zebrafish embryos has been shown to contribute to heart and jaw malformation phenotypes. The mechanisms by which AHR2 (functional ortholog of mammalian AHR) activation leads to reduced *sox9b* expression levels and subsequent target organ toxicity are unknown. We have identified a novel long non-coding RNA (*slincR*) that is upregulated by strong AHR ligands and is located adjacent to the *sox9b* gene. We hypothesize that *slincR* is regulated by AHR2 and transcriptionally represses *sox9b.* The *slincR* transcript functions as an RNA macromolecule, and *slincR* expression is AHR2-dependent. Antisense knockdown of *slincR* results in an increase in *sox9b* expression during both normal development and AHR2 activation, which suggests a relief in repression. During development, *slincR* was expressed in tissues with *sox9* essential functions, including the jaw/snout region, otic vesicle, eye, and brain. Reducing the levels of *slincR* resulted in altered neurological and/or locomotor behavioral responses. Our results place *slincR* as an intermediate between AHR2 activation and the reduction of *sox9b* mRNA in the AHR2 signaling pathway.

Molecular Pharmacology Fast Forward. Published on April 6, 2017 as DOI: 10.1124/mol.117.108233
This article has not been copyedited and formatted. The final version may differ from this version.



## INTRODUCTION

The zebrafish (*Danio rerio*) model has proven to be an invaluable tool in multiple areas of research, such as development and toxicology (Dooley and Zon, 2000; Garcia et al., 2016; Spitsbergen and Kent, 2003). The anatomy and physiology of fish is homologous to humans (Ackermann and Paw, 2003). 84% of human disease-related genes are present in the zebrafish genome, and about 70% of human genes have a zebrafish ortholog (Howe et al., 2013). The zebrafish has been used as a model to elucidate the molecular mechanisms responsible for 2,3,7,8-tetrachlorodibenzo-*p*-dioxin (TCDD) toxicity (Henry et al., 1997). In zebrafish, developmental exposure to TCDD causes impaired reproductive development, embryonic lethality, and/or severe developmental defects in several tissues, including heart, cartilage, and vasculature (reviewed in Carney et al., 2006).

TCDD toxicity is mediated through the aryl hydrocarbon receptor (AHR) (reviewed in Beischlag et al., 2008). The AHR is a conserved receptor from invertebrates upwards and is the only ligand-activated member of the basic helix-loop-helix PER-ARNT-SIM protein family (Hahn et al., 1997; Hao and Whitelaw, 2013). The AHR can be activated by many environmental contaminants, including chlorinated dioxins, biphenyls, and polyaromatic hydrocarbons (Knecht et al., 2013; Wall et al., 2015). Upon activation, AHR dimerizes with the aryl hydrocarbon nuclear translocator (ARNT), translocates to the nucleus, and induces ligand-specific transcriptional changes (Beischlag et al., 2008; Goodale et al., 2015). In zebrafish, AHR2 and ARNT1 are the functional orthologs of mammalian AHR and ARNT, and loss of either protein protects against TCDD-induced toxicity phenotypes, including cardiac malformation, cartilage malformation, and reduced peripheral blood flow (Antkiewicz et al., 2006; Prasch et al., 2006).

Identification of the downstream molecular targets responsible for specific endpoints of AHR-dependent toxicity remain largely unknown; however, in zebrafish, SRY-type box 9b (*sox9b*) has been identified as one of the most reduced transcripts in several AHR2 toxicity target organs (Andreasen et al., 2007; Andreasen et al., 2006; Hofsteen et al., 2013; Xiong et al., 2008). In

Molecular Pharmacology Fast Forward. Published on April 6, 2017 as DOI: 10.1124/mol.117.108233
This article has not been copyedited and formatted. The final version may differ from this version.



zebrafish, an ancient genome duplication in the teleost lineage resulted in two *Sox9* co-orthologs (*sox9a* and *sox9b*), which have undergone subfunction partitioning with both distinct and overlapping functions (Postlethwait et al., 2004; Yan et al., 2005). *Sox9* is required for proper vertebrate embryonic development by specifying cell fate and differentiation in linages from all three germ layers (Akiyama et al., 2004; Akiyama et al., 2002; Furuyama et al., 2011; Haldin and LaBonne, 2010; Scott et al., 2010; Stolt and Wegner, 2010).

*Sox9b* is hypothesized to have a causal role in cartilage and heart TCDD-induced toxicity phenotypes in zebrafish. Antisense knockdown of *sox9b* was sufficient to produce the TCDD-like jaw phenotype, and TCDD-exposed zebrafish embryos injected with *sox9b* mRNA rescued the TCDD-induced jaw malformations (Xiong et al., 2008). TCDD exposure markedly reduces the expression of *sox9b* in zebrafish heart ventricles, and genetic ablation of *sox9b* results in TCDD-like heart malformations (Hofsteen et al., 2013). The Xiong and Hofsteen studies indicate the reduction in *sox9b* expression is partially responsible for the TCDD-induced cartilage and heart malformation phenotypes. While eight putative AHREs are located within 5 kb of the *sox9b* transcriptional start site, *sox9b* downregulation does not occur until 4 hours after AHR2 activation, suggesting *sox9b* is not a direct AHR2 target gene (Xiong et al., 2008). The mechanisms by which AHR2 activation leads to a reduction in *sox9b* expression and subsequent target organ toxicity are unknown.

Long non-coding RNAs (lncRNAs) are defined as transcripts equal to or greater than 200 nucleotides that do not appear to encode a protein. Genetic and biochemical evidence suggest that a primary role for lncRNAs is the regulation of epigenetic processes, most likely by guiding chromatin-modifying enzymes to their target sites and by acting as a platform for chromosomal organization and protein complexes (Quinn and Chang, 2016). LncRNAs have been implicated in an array of biological processes, including embryonic viability, development, response to stress, and cancer metastasis (Fatica and Bozzoni, 2014; Gutschner and Diederichs, 2012).

Molecular Pharmacology Fast Forward. Published on April 6, 2017 as DOI: 10.1124/mol.117.108233
This article has not been copyedited and formatted. The final version may differ from this version.



An important question left unanswered is how AHR2 activation by an exogenous ligand leads to the reduction of *sox9b* expression. We used the zebrafish model to probe the relationship between AHR2, a novel lncRNA (*slincR*), and *sox9b*. *SlincR* is located adjacent to the *sox9b* gene locus, and *slincR* expression was increased by a strong AHR ligand, which led us to test the hypothesis that *slincR* is regulated by AHR2 and is required for proper *sox9b* expression levels.

Molecular Pharmacology Fast Forward. Published on April 6, 2017 as DOI: 10.1124/mol.117.108233
This article has not been copyedited and formatted. The final version may differ from this version.



## MATERIALS AND METHODS

All gene-specific primers, *in situ* probes, and antibody information is listed in (Supplemental Table 1).

### *Fish husbandry*

Tropical 5D (wild type) and the *Tg*(*−2421/ +29sox9b:EGFP*$_{uw2}$) *sox9b* reporter strains of zebrafish (*Danio rerio*) were reared according to Institutional Animal Care and Use Committee protocols at the Sinnhuber Aquatic Research Laboratory, Oregon State University. Adult fish were raised in a recirculating water system (28 ± 1°C) with a 14-h:10-h light-dark schedule. Spawning and embryo collection were conducted as described in (Westerfield, 2007).

### *Waterborne exposure*

Shield-stage (~6 hpf) embryos were exposed to 1 ng/mL TCDD (311 nM, 95.3% purity; SUPELCO Solutions Within; Bellfonte, PA) or vehicle (0.1% DMSO) with gentle rocking for 1 hour in 20 mL glass vials (10 embryos/mL). Vials were also gently inverted every 15 minutes to ensure proper mixing. After the exposure, embryos were rinsed 3 times with fish water and then raised in 100-mm petri dishes. We developmentally exposed embryos to 10 μM B[*a*]AQ as described in (Goodale et al., 2015).

### *5' and 3' rapid amplification of cDNA ends*

The FirstChoice RLM-RACE kit was performed as recommended by manufacturer (Thermo Fisher; Eugene, OR). RNA was isolated at 48 hpf from whole embryos and cDNA was synthesized as described below. Sanger sequencing was performed by the Core Facilities of the Center for Genome Research and Biocomputing at Oregon State University using an ABI 3730 capillary sequence machine.

### *Embryo homogenization and subcellular fractionation*

Approximately 50-60 embryos at 4 days post fertilization were homogenized with a 2 mL dounce homogenizer and tight pestle, and fractionated with a glucose gradient and centrifugation as detailed in (Bogdanovic et al., 2013). The homogenization solutions followed the recipes

Molecular Pharmacology Fast Forward. Published on April 6, 2017 as DOI: 10.1124/mol.117.108233
This article has not been copyedited and formatted. The final version may differ from this version.



described in (Simon, 2013). For each cellular compartment, total RNA was isolated and cDNA was synthesized and quantified as described below; however, only 2 ng of cDNA was used per reaction, the samples were not normalized to a reference gene and whole embryo homogenate served as the calibrator. Samples analyzed consist of 3 biological replicates, and 2 technical replicates. *U1* rRNA served as a positive controls for nuclear enrichment.

***Selective 2'-hydroxyl acylation analyzed by primer extension (SHAPE)***

Details of the experimental methods are summarized in (Kladwang et al., 2011). Wild type RNA reference ladders were created using 3′dideoxy-TTP in an equilmolar amount to dTTP during the reverse transcription reaction. The SHAPE data were analyzed using HiTRACE-WEB (Kim et al., 2013). Replicates from three independent samples were compared, and we performed a signal decay correction step to normalize for the typical exponential decay in fluorescent intensity as a function of elution time (Karabiber et al., 2013). We normalized each point by dividing by the average intensity of positions later in elution time (earlier in nucleotide position), rather than the sum, because in practice the sum overcorrected for the signal decay. We then averaged the replicates and computed the probability of an adduct $p_{add}$, by subtracting the scaled average DMSO from the average NMIA signal to remove background noise (Karabiber et al., 2013). We fit the data to a normal distribution and capped the data above the 90th percentile to control any signal that was likely due to saturation. Lastly, we scaled the data to be between 0 and 2 (Karabiber et al., 2013; Vasa et al., 2008). The secondary structure was computed with RNAfold, excluding isolated pairs, using dangling energies on both sides of helices, and the “Turner 2004” energy parameters (Lorenz et al., 2011; Turner and Mathews, 2010). Folding was performed at 24 °C, in accordance with experimental conditions, and SHAPE reactivities were used in the calculation using the Deigan algorithm with default parameters (Deigan et al., 2009).

***Morpholino injection***

Approximately 2 nl total volume of a 1 mM solution of each morpholino (MO) were microinjected in the yolk of wild type 5D and *sox9b*-eGFP reporter embryos at the one-cell stage.

Molecular Pharmacology Fast Forward. Published on April 6, 2017 as DOI: 10.1124/mol.117.108233
This article has not been copyedited and formatted. The final version may differ from this version.



To test the effect of knocking down *slincR* expression levels, a splice blocking MO targeting the exon/intron boundary of *slincR* exon 1 (*slincR*-MO: 5′ GAC CTA AAC TCG ACC TTA CCA GAT C 3′) and a standard negative control (ConMO: 5′ CCT CTT ACC TCA GTT ACA ATT TAT A 3′) were obtained from GeneTools, Philomath, OR. Two methods were used to validate knockdown efficiencies: total RNA was isolated and cDNA was synthesized and quantified, and/or *in situ* hybridization using a *slincR* probe (both detailed below).

***RNA extraction and mRNA quantification***

Total RNA was extracted from 48 hpf whole embryos using RNAzol (Molecular Research Center, Inc; Cincinnati, OH) and a bullet blender with 0.5 mM zirconium oxide beads (Next Advance; Averill Park, New York) as recommended by the manufacturer. RNA quality and quantity was assessed using a SynergyMix microplate reader with the Gen5 Take3 module. Each biological sample consisted of 20 embryos with a minimum of 3 biological replicates per condition. Total RNA (1 µg) was reverse transcribed into cDNA with random primers using the ABI High-Capacity cDNA Reverse Transcription Kit (Thermo Fisher; Eugene, OR). Quantitative real-time PCR (qRT-PCR) was performed using a StepOnePlus Real-Time PCR System (Applied Biosystems; Foster City, CA). The 20 µl reactions consisted of 10 µl 2X SYBR Green Master Mix (Roche; Pleasanton, CA), 0.4 µl each of 10 µM forward and reverse primers, and 20 ng cDNA. Expression values were normalized to β-*actin* and analyzed with the $2^{-\Delta\Delta CT}$ method as described in (Livak and Schmittgen, 2001). Results were statistically analyzed using GraphPad Prism 7.02 software. The data were tested for normality using the Shapiro-Wilk normality test and analyzed with a two-way ANOVA, and a correction for multiple comparisons was performed using the Dunnett's test (95% confidence intervals) or a paired *t*-test and corrected for multiple comparison using the Holm-Sidak method, with $\alpha$ = 0.05. Error bars indicate SD of the mean. We used the following calculation to determine morpholino knockdown efficiencies (%KD = (1 – ΔΔCT) * 100%). All experiments were independently repeated a minimum of 2 times.

**In situ *hybridization and immunohistochemistry***

Molecular Pharmacology Fast Forward. Published on April 6, 2017 as DOI: 10.1124/mol.117.108233
This article has not been copyedited and formatted. The final version may differ from this version.



*In situ* localization of RNA was performed on whole embryos (*n* = 6-10 embryos) at the respective time points, as described previously (Thisse and Thisse, 2008), with the exception that the embryos were permeabilized in 2% hydrogen peroxide in 100% methanol for 20 minutes prior to the initial embryo rehydration. Additionally, probes were hybridized in a final concentration of 10% dextran sulfate. The *sox9b* probe was obtained from (Chiang et al., 2001). The *slincR*, *notch3*, and *adamts3* probes were prepared by PCR amplification from cDNA template as described in (Thisse and Thisse, 2008). Dual *in situ* hybridization and immunohistochemistry samples were performed on the *Tg*(*−2421/+29sox9b:EGFP*$_{uw2}$) *sox9b* reporter line. Embryos were imaged in 3% methylcellulose at room temperature using a Keyence BZ-x700 at 10X with 0.45 aperture and processed with the BZ-x Analyzer software.

***Larval morphology and behavior screen***

Zebrafish embryos were injected at the 1-cell stage with morpholinos as described above and placed into 96-well plates after hatching (~48-60 hpf), with 24 embryos per injection group. The larval photomotor response (LPR) assay consisted of 3 min light and dark alternating periods, for a total of four light-dark transitions, with the first transition representing an acclimation period. The Viewpoint Zebrabox systems (Viewpoint Behavior Technology) were used to analyze photo-induced larval locomotor activity in 120 hpf larvae. We followed the protocols and analyzed the overall area under the curve for the last three light-dark cycles compared to control morphants using a Kolmogorov-Smirnov test ($p < 0.01$) as described in (Knecht et al., 2016). We utilized a 1% alpha to control for type I error inflation rather than controlling the family-wise error rate as we are not correcting for multiple treatments, but only a control and treatment group. Zebrafish were evaluated at 120 hpf for mortality and a suite of 17 physical malformations prior to the viewpoint assay, and embryos identified to be malformed were excluded from the viewpoint data analysis (Truong et al., 2011). The morphology data is analyzed using a Fisher's exact test because of its utility of low category counts, and it does not make distributional assumptions (as chi-squared test

Molecular Pharmacology Fast Forward. Published on April 6, 2017 as DOI: 10.1124/mol.117.108233
This article has not been copyedited and formatted. The final version may differ from this version.



does). A Bonferroni multiple comparison to control for family-wise error rate was used. The experiment was performed two independent times.

Molecular Pharmacology Fast Forward. Published on April 6, 2017 as DOI: 10.1124/mol.117.108233
This article has not been copyedited and formatted. The final version may differ from this version.



## RESULTS

### *Molecular characterization of* slincR

We previously performed an RNA-sequencing experiment on 48 hpf whole embryos treated with a strong AHR2 ligand (10 μM benz(*a*)anthracene-7-12-dione; B[*a*]AQ) to identify the transcriptional networks of protein coding genes that are regulated by AHR2 (Goodale et al., 2015). Recent advances in our ability to measure RNA transcripts have unveiled lncRNAs as important regulators of gene expression (Quinn and Chang, 2016). We mined the data from the Goodale study in an effort to discover potential lncRNAs that are regulated by AHR2. Using Ensembl's zebrafish genome build Zv9 (release 79), we identified a novel transcript that displayed a log2 fold increase of 3.2 upon developmental exposure to 10 μM B[*a*]AQ. A portion of the novel transcript matched the Ensembl annotated lncRNA *si:Ch1073-384e4.1,* which is located adjacent to the *sox9b* gene on the opposite strand of chromosome 3. The large increase in expression in response to a strong AHR2 ligand and the close proximity to the *sox9b* locus led us to hypothesize that *si:Ch1073-384e4.1* may be regulated by AHR2 and transcriptionally represses *sox9b*. Using 5′ and 3′ rapid amplification of cDNA ends and sequencing analysis, the transcript we identified partially overlaps with the Ensembl annotated lncRNA, *si:Ch1073-384e4.1*. This novel transcript, ***s****ox9b* **l**ong **i**ntergenic **n**on-**c**oding **R**NA (*slincR*, Genbank accession number KY085961), shares a 57.6% identity with *si:Ch1073-384e4.1*, with a majority of the similarities found in exon 1 of both transcripts (data not shown). *SlincR* is 466 bp in length, contains 3 exons, and is polyadenylated (Figure 1A). We were unable to consistently amplify the Ensembl *si:Ch1073-384e4.1* transcript in whole embryos treated with DMSO or B[*a*]AQ (data not shown). We note that *si:Ch1073-384e4.1* and *slincR* represent alternative splice variants; however, *slincR* appears to be the most abundant transcript in our fish population. The core AHR responsive element (AHRE, 5′-T/GCGTG-3′) is present in multiple locations in the *slincR* promoter, suggesting *slincR* may be a direct AHR target gene (Figure 1A). When comparing the zebrafish *slincR-sox9b* loci to that of the mouse and human genome, the spatial arrangement and orientation of potential *slincR* orthologs relative to

Molecular Pharmacology Fast Forward. Published on April 6, 2017 as DOI: 10.1124/mol.117.108233
This article has not been copyedited and formatted. The final version may differ from this version.



*Sox9* and the presence of AHREs in the promoters of the potential orthologs is conserved. Thus, we expect the lncRNA-*Sox9* target relationship to be similar between fish and mammals.

To determine the cellular compartment(s) in which *slincR* is localized, we homogenized ~50-60 whole embryos at 96 hpf, and then used standard centrifugation fractionation methods, followed by qRT-PCR. There is no significant difference in the relative amounts of *slincR* located in the nucleus versus the cytoplasm. (Figure 1B). Previous reports have demonstrated that quantitative, nucleotide resolution information from a selective 2'-hydroxyl acylation, analyzed by primer extension (SHAPE) experiment, can result in RNA secondary structure predictions with accuracies up to 96-100% (Deigan et al., 2009). Briefly, SHAPE allows the probing of RNA secondary structures at single-nucleotide resolution by incubating RNA with *N*-methylisatoic anhydride, which selectively modifies flexible nucleotides and inhibits reverse transcription. The RNA is reverse transcribed, and modified bases are detected via capillary electrophoresis; thus, the SHAPE reactivity data can discriminate between base-paired versus unconstrained or flexible nucleotides in a RNA molecule. We used SHAPE-generated pseudo-free energies, in conjunction with RNAfold, to increase the accuracy of *slincR*'s predicted secondary structure (Figure 1C). We scaled the data to be between 0 and 2 and entered the SHAPE reactivities into RNAfold. Unreactive nucleotides (white) participate in canonical base pairs; whereas, nucleotides in loops, bulges, and other connecting regions are reactive (blue). The tertiary structure is an additional level of information that is required to understand *slincR*'s structure and function relationship.

**SlincR *and* sox9b *are expressed in adjacent and overlapping tissues through multiple stages of development***

In order to better understand endogenous functions of *slincR*, we investigated expression relative to *sox9b* with *in situ* hybridization in embryos of the wild type and *sox9b*-eGFP reporter lines over multiple developmental time points (24, 36, 48, 60 and 72 hpf). *SlincR* expression was not detectable at 24 hpf, but starting at 36 hpf expression was evident in the otic vesicle, eye, and jaw/snout region (Table 1). *Sox9b*-eGFP and *slincR* were expressed in adjacent and overlapping

Molecular Pharmacology Fast Forward. Published on April 6, 2017 as DOI: 10.1124/mol.117.108233
This article has not been copyedited and formatted. The final version may differ from this version.



tissues, including the eye, otic vesicle, and lower jaw region during multiple stages of development (Figure 2A and B).

**SlincR *expression is AHR2-dependent***

To test our hypothesis that activation of AHR2 results in an increase in *slincR* expression, we used the previously characterized AHR2-null zebrafish line (Goodale et al., 2012). In 48 hpf wild type samples, *slincR* expression was significantly increased upon exposure to TCDD (Figure 3A). In AHR2-null animals, however, *slincR* expression was significantly lower compared to wild type at 48 hpf, and no increase in *slincR* expression was observed after developmental exposure to TCDD (Figure 3A). These results demonstrate that *slincR* expression is increased by exposure to strong AHR ligands (B[*a*]AQ and TCDD) and that this induction is an AHR2-dependent event.

To elucidate the changes in the spatial expression pattern of *slincR* relative to *sox9b* upon AHR2 activation, we exposed the previously characterized *sox9b*-eGFP reporter line *Tg*(*−2421/+29sox9b:EGFP*$_{uw2}$) to 0.1% DMSO or 1 ng/mL TCDD, and performed dual IHC and *in situ* hybridization (Plavicki et al., 2014). Exposure to TCDD displayed decreased *slincR* expression in the brain and increased expression surrounding the otic vesicle, relative to vehicle-exposed samples (Figure 3B). In the TCDD-exposed samples, the regions with increased *slincR* expression had a corresponding decrease in *sox9b*-eGFP expression (Figure 3B, white rectangle). The *slincR* expression pattern was similar in all fish examined within each treatment group (Supplemental Figure 1). Of note, exposure to TCDD also resulted in *slincR* expression in the pectoral fin, which was not seen in DMSO treated samples (Figure 3B). Interestingly, the 0.1% DMSO (vehicle control) exposed embryos displayed increased *slincR* expression in the brain compared to TCDD-exposed. The non-exposed (DMSO or TCDD) embryos did not show any expression of *slincR* in the brain (Figure 3 and Table 1). The specific and overlapping expression patterns suggest, but do not prove, interaction between *sox9b* and *slincR*.

**SlincR *is required for proper expression levels and spatial pattern of* sox9b *during development***

Molecular Pharmacology Fast Forward. Published on April 6, 2017 as DOI: 10.1124/mol.117.108233
This article has not been copyedited and formatted. The final version may differ from this version.



To probe the *slincR-sox9b* relationship during development antisense knockdown of the endogenous *slincR* and splice variant *si:Ch1073-384e4.1* levels via a splice blocking morpholino was performed (Figure 4A). We tested knockdown efficiencies in 48 hpf *slincR* morphants exposed to DMSO or TCDD, which displayed 98% and 81% knockdown efficiencies, respectively (Figure 4A). *In situ* hybridization of *slincR* from 48 and 72 hpf (Figure 4C and 4D) control morphant samples exposed to TCDD shows that *slincR* expression is increased in the otic vesicle and the lower jaw/snout region. *In situ* hybridization also confirmed that *slincR* was barely detected in *slincR* morphants at 48 hpf when treated with DMSO; however, expression of *slincR* was visible in the otic vesicle and lower jaw region in the TCDD-treated samples (Supplemental Figure 2). Knockdown of *slincR* during early development was not sufficient to rescue the TCDD-induced cartilage malformation phenotype. As previously mentioned, activation of AHR2 by TCDD exposure results a reduction in the expression of *sox9b* mRNA in craniofacial cartilage, regenerating caudal fin, and heart tissues (Andreasen et al., 2007; Andreasen et al., 2006; Hofsteen et al., 2013; Xiong et al., 2008); therefore, we hypothesized that upon exposure to a strong AHR2 ligand, *slincR* increases and is required for the TCDD-mediated reduction in *sox9b* expression. To determine if *slincR* expression was required for the reduction of *sox9b* mRNA in TCDD-treated embryos, we exposed control and *slincR* morphants to 0.1% DMSO or 1 ng/mL TCDD, isolated RNA from whole embryos at 48 hpf, and then measured the relative expression levels of *sox9b* mRNA. In control morphants, exposure to TCDD resulted in a decrease in *sox9b* mRNA levels (Figure 4B). In contrast, the *slincR* morphants exposed to either DMSO or TCDD displayed a significant increase in *sox9b* expression compared to the control morphants (Figure 4B). Next, we used *in situ* hybridization to label *sox9b* mRNA in 48 hpf *slincR* and control morphants exposed 0.1% DMSO or 1 ng/mL TCDD. *SlincR* morphants exposed to DMSO displayed an increase in *sox9b* expression in the otic vesicle and midbrain region compared to DMSO-exposed controls (Figure 4E). In response to TCDD exposure, *slincR* morphants also displayed an increase in *sox9b* expression in the otic vesicle, lower jaw/snout region, and eye

Molecular Pharmacology Fast Forward. Published on April 6, 2017 as DOI: 10.1124/mol.117.108233
This article has not been copyedited and formatted. The final version may differ from this version.



compared to control morphants (Figure 4E and F). The data suggest that *slincR* is required for normal *sox9b* expression levels and for the TCDD-mediated reduction in *sox9b* expression.

Knocking down *slincR* expression altered *sox9b* mRNA transcript levels (Figure 4B) and spatial expression pattern (Figure 4E and 4F). Next we determined if the increased expression of *sox9b* observed in the *slincR* morphants had a significant effect on known *sox9b* downstream target genes. We selected genes that were experimentally identified as direct *Sox9* target genes in mammalian primary chondrocytes via a ChIP-seq experiment and examined the orthologous genes in our zebrafish model (Ohba et al., 2015). In the *slincR* morphants, 5 out of the 9 genes selected had significantly altered relative expression levels at 48 hpf compared to the control (Figure 5A). The transcripts for *notch3*, *adamts3*, *sfrp2*, and *fgfr3* all had an increase in expression in *slincR* morphants, while *fabp2* displayed a decrease in expression compared to controls. To identify the tissues/regions with altered expression patterns, we used *in situ* hybridization to label *notch3* and *adamts3* (a protease that cleaves notch) mRNA in 48 hpf *slincR* and control morphants (Figure 5B and 5C). Similar to the *slincR* and *sox9b* expression patterns, *notch3* and *adamts3* are also expressed in the lower jaw/snout region, eye, otic vesicle, and brain at 48 hpf. *SlincR* morphants clearly displayed an increase in *notch3* expression in the midbrain, hindbrain, eye, and pectoral fin and increased *adamts3* expression in the somites of the trunk. These results suggest *slincR* knockdown had a modest, but significant impact on the *sox9b* transcriptional regulatory network across multiple tissues during development.

***SlincR expression is required for normal neurological and/or locomotor behavioral responses to light***

We used an 18 endpoint viability and malformation screen on 120 hpf fish ($n$ = 24) to determine the morphological impact of knocking down *slincR* expression levels early in development. Reduced *slincR* expression levels during development did not result in any statistically significant malformation incidences at 120 hpf (Figure 6A). Morphologically, the *slincR* morphants were indistinguishable from control morphants, with both appearing developmentally

Molecular Pharmacology Fast Forward. Published on April 6, 2017 as DOI: 10.1124/mol.117.108233
This article has not been copyedited and formatted. The final version may differ from this version.



normal. To evaluate the effect of reduced *slincR* expression levels on neurological and locomotor behavior, 120 hpf fish ($n$ = 23) were subjected to a light-dark photometer assay that reported hyperactive or hypoactive swimming (Knecht et al., 2016). The morphological and behavioral assays were conducted on the same 120 hpf fish. Reducing *slincR* expression during early development resulted in a modest but significantly hypoactive photomotor response ($p < 0.01$; -14.04% difference in mean AUC compared to controls; Figure 6B). The LPR assay suggested that reduced *slincR* expression significantly affected some aspect(s) of neuromuscular and/or sensory system development.

Molecular Pharmacology Fast Forward. Published on April 6, 2017 as DOI: 10.1124/mol.117.108233
This article has not been copyedited and formatted. The final version may differ from this version.



## DISCUSSION

The aryl hydrocarbon receptor is a key mediator of cell signaling during development and homeostasis, as well as in response to environmental pollutant exposure (Hao and Whitelaw, 2013). Dysregulation of AHR has been associated with multiple diseases, such as coronary artery and prostrate disease (Huang et al., 2015; Schneider et al., 2014; Vezina et al., 2009). In humans, haploinsufficiency of *SOX9* is associated with organ malformations, while *SOX9* duplication results in male-to-female sex reversal (Huang et al., 1999). Increased or ectopic expression of *SOX9* is associated with liver fibrosis and several different cancer types (Matheu et al., 2012; Pritchett et al., 2011). *Sox9* plays an important role during embryonic development, determining cell fate in cells derived from all three germ layers (Jo et al., 2014). Recent work has also suggested a role for *Sox9* in cell maintenance and specification during adulthood (Barrionuevo et al., 2016; Furuyama et al., 2011). Our study examined the relationship between AHR2, a novel lncRNA (*slincR*), and *sox9b* using the zebrafish model, in order to gain insight into how inappropriate AHR2 activation leads to a reduction in *sox9b* expression and impairs cartilage and heart development. Understanding the layers of regulation downstream of AHR will aid our understanding of the role of AHR in development and how xenobiotic activation or misexpression of AHR leads to negative phenotypic consequences.

The results of this study suggest that *slincR* expression is AHR2-dependent and is required for proper *sox9b* expression levels during normal development. *Sox9b* is hypothesized to have a causal role in the AHR2 toxicity signaling pathway, since antisense knockdown of *sox9b* was sufficient to phenocopy TCDD–induced craniofacial cartilage malformations (Xiong et al., 2008). Additionally, a *sox9b* mutant partially phenocopied AHR2-activated cardiac malformations in zebrafish, indicating *sox9b* and other unidentified genes are responsible for the heart malformation phenotype (Hofsteen et al., 2013). In the absence of functional AHR2, *slincR* expression was significantly lower than in wild type fish and did not increase in response to TCDD exposure. Additionally, when we knocked down the levels of *slincR* and activated the AHR2

Molecular Pharmacology Fast Forward. Published on April 6, 2017 as DOI: 10.1124/mol.117.108233
This article has not been copyedited and formatted. The final version may differ from this version.



pathway, we did not see a reduction in *sox9b* expression. These results place *slincR* as an intermediate between AHR2 activation and the reduction of *sox9b* expression in the AHR signaling pathway.

In support of a relationship between *slincR* and *sox9b*, *slincR* was shown to be expressed in adjacent and overlapping tissues and have a significant impact on the expression of *sox9b* and several of its downstream targets. Our data demonstrate that the *slincR* transcript functions as an RNA macromolecule and acts locally (in *cis*) on chromosome 3 to regulate the spatial and relative expression levels of *sox9b*. We detected *slincR* expression in tissues that have reported essential functions for *sox9*, including the otic vesicle, eye, and brain (Scott et al., 2010; Yan et al., 2005; Zhu et al., 2013). Upon TCDD exposure, *sox9b* expression is reduced in zebrafish heart ventricles (Hofsteen et al., 2013). We did not detect *slincR* in the developing heart, which suggests there are tissue specific mechanisms of *sox9b* regulation. In *slincR* morphants, we detected significant differences in the relative expression levels of *sox9b* and known *Sox9* targets that were previously identified in mammalian primary chondrocytes. Several of the significantly altered genes are also known to converge with *Sox9* signaling in multiple organs through development, including *fgf3*, *sfrp2* (Wnt ligand), and *notch3* (Jo et al., 2014). In *slincR* morphants, *notch3* and *adamts3* (protease that cleaves notch receptors), both had a small but significant increase in their relative expression and displayed altered spatial expression patterns. In cartilage development, notch signaling has been shown to regulate the onset of chondrocyte maturation in a *Sox9*-dependent manner and negatively regulate chondrocyte differentiation by suppressing *Sox9* transcription (Kohn et al., 2015). Evidence from mouse chondrogenic ATDC5 cells suggests that notch signaling initially induces *Sox9* expression, but prolonged notch signaling leads to suppression of *Sox9* transcription via secondary effectors (Chen et al., 2013). Notch signaling in ectoderm-derived cells, which includes the central nervous system, otic placode, and eye, was shown to induce *sox9* expression for stem cell maintenance, astrogliogenesis, and eye development (Martini et al., 2013; Zhu et al., 2013).

Molecular Pharmacology Fast Forward. Published on April 6, 2017 as DOI: 10.1124/mol.117.108233
This article has not been copyedited and formatted. The final version may differ from this version.



In our study, reducing the expression of *slincR* during early stages of development did not result in overt malformations at the organismal level. These results are not surprising for a number of reasons. In zebrafish, a phenotypic analysis of 1,216 non-sense and essential splice mutations resulted in 87.58% of mutations linked to no observable morphological or behavioral phenotype. This implies that the zebrafish genome operates under a high degree of redundancy and may indicate the presence of genetic compensatory networks (Kettleborough et al., 2013). Additionally, we hypothesize that *slincR* expression is downstream of AHR2, and the AHR2-null line does not display overt malformations during embryonic development (Goodale et al., 2012).

A reduction in *slincR* expression during early stages of embryonic development resulted in altered photomotor responses. We also detected *slincR* expression in the brain of DMSO and TCDD-exposed embryos. DMSO is known to cause membrane destabilization and has been used to facilitate administration of drugs that do not normally cross the blood brain barrier (Kleindienst et al., 2006; Pardridge, 2005). *SlincR* expression in the brain was not seen in DMSO-exposed AHR2-null mutants. It is plausible that exposure to DMSO decreased the integrity of the blood brain barrier, allowing an unidentified ligand to activate the AHR2 receptor in the brain. *SlincR* morphants also displayed altered *sox9b* and *notch3* expression patterns in the brain. Mammalian and zebrafish models have identified a large number of lncRNAs that exhibit neuronal-specific expression, which suggest a role for lncRNAs in the establishment and maintenance of the vertebrate nervous system (Kaushik et al., 2013; Mercer et al., 2008). In the adult zebrafish, the largest number of tissue specific lncRNA transcripts were expressed in the brain (Kaushik et al., 2013). In mammals and zebrafish, *Sox9* is expressed in the brain and is a conserved transcription factor involved in CNS development (Esain et al., 2010; Martini et al., 2013; Plavicki et al., 2014; Scott et al., 2010).

Our study did not address how *slincR* expression leads to reduced *sox9b* mRNA levels. Future studies will be conducted to establish the mechanism of *slincR*-induced *sox9b* suppression. A limitation of this study was our inability to maintain *slincR* repression during later

Molecular Pharmacology Fast Forward. Published on April 6, 2017 as DOI: 10.1124/mol.117.108233
This article has not been copyedited and formatted. The final version may differ from this version.



stages of development to determine late-stage phenotypic consequences. This prevented us from determining *slincR*'s contribution to TCDD-induced toxicity phenotypes, such as cartilage malformation. Knocking down *slincR* during early development is not sufficient to rescue the TCDD-induced cartilage malformation phenotype. In future studies, we will use a CRISPR/Cas9-generated *slincR* knockout line and increase the resolution by examining the tissues and cells in which *slincR* is expressed.

In summary, we identified an AHR2-dependent novel long non-coding RNA (*slincR*) that is required for proper *sox9b* expression during normal development and in response to a strong AHR ligand. *SlincR* acts in *cis* to regulate *sox9b* expression; however, additional experiments are required to determine the mechanism of *slincR*-induced reduction of *sox9b*. In concordance with other lncRNA studies, *slincR* expression was tissue-specific and was not required for normal morphological development (measured at the organismal level). *SlincR* was required for normal photomotor behavior in the larval stage, suggesting a role for *slincR* in neuromuscular and/or sensory system development. This study adds to the growing body of research demonstrating important roles of lncRNAs during neural development, and adds to our understanding of how AHR signaling intersects with the *sox9b* network to mediate developmental effects of environmental pollutants.

Molecular Pharmacology Fast Forward. Published on April 6, 2017 as DOI: 10.1124/mol.117.108233
This article has not been copyedited and formatted. The final version may differ from this version.



## ACKNOWLEDGMENTS

**Acknowledgments**: The *slincR* transcript sequence has been deposited into Genbank (accession number KY085961). We thank Dr. Michael Simonich and Cheryl Dunham for help with editing the manuscript. We would also like to thank the agents of SARL, especially Carrie Barton and Greg Gonnerman, for all their help regarding fish husbandry and phenotypic screening. We also acknowledge Dr. Lisa Truong for her assistance with data analysis. The *Sox9b* reporter line *Tg*(*−2421/+29sox9b:EGFP*$_{uw2}$) was generously provided by the Richard E. Peterson Lab from the University of Wisconsin-Madison, Madison, WI, USA.

Molecular Pharmacology Fast Forward. Published on April 6, 2017 as DOI: 10.1124/mol.117.108233
This article has not been copyedited and formatted. The final version may differ from this version.



## AUTHOR CONTRIBUTIONS

*Participated in research design:* Tanguay, Hendrix, Garcia, and Goodale

*Conducted experiments:* Goodale, Garcia, and La Du

*Performed data analysis:* Hendrix, Wiley, Garcia, and Goodale

*Wrote or contributed to the writing of the manuscript:* Goodale, Garcia, La Du, and Tanguay

**REFERENCES**

Ackermann GE and Paw BH (2003) Zebrafish: a genetic model for vertebrate organogenesis and human disorders. *Front Biosci* **8**: d1227-1253.

Akiyama H, Chaboissier MC, Behringer RR, Rowitch DH, Schedl A, Epstein JA and de Crombrugghe B (2004) Essential role of Sox9 in the pathway that controls formation of cardiac valves and septa. *Proc Natl Acad Sci U S A* **101**(17): 6502-6507.

Akiyama H, Chaboissier MC, Martin JF, Schedl A and de Crombrugghe B (2002) The transcription factor Sox9 has essential roles in successive steps of the chondrocyte differentiation pathway and is required for expression of Sox5 and Sox6. *Genes Dev* **16**(21): 2813-2828.

Andreasen EA, Mathew LK, Lohr CV, Hasson R and Tanguay RL (2007) Aryl hydrocarbon receptor activation impairs extracellular matrix remodeling during zebra fish fin regeneration. *Toxicol Sci* **95**(1): 215-226.

Andreasen EA, Mathew LK and Tanguay RL (2006) Regenerative growth is impacted by TCDD: gene expression analysis reveals extracellular matrix modulation. *Toxicol Sci* **92**(1): 254-269.

Antkiewicz DS, Peterson RE and Heideman W (2006) Blocking expression of AHR2 and ARNT1 in zebrafish larvae protects against cardiac toxicity of 2,3,7,8-tetrachlorodibenzo-p-dioxin. *Toxicol Sci* **94**(1): 175-182.

Barrionuevo FJ, Hurtado A, Kim GJ, Real FM, Bakkali M, Kopp JL, Sander M, Scherer G, Burgos M and Jimenez R (2016) Sox9 and Sox8 protect the adult testis from male-to-female genetic reprogramming and complete degeneration. *Elife* **5**.

Beischlag TV, Luis Morales J, Hollingshead BD and Perdew GH (2008) The aryl hydrocarbon receptor complex and the control of gene expression. *Crit Rev Eukaryot Gene Expr* **18**(3): 207-250.

Bogdanovic O, Fernandez-Minan A, Tena JJ, de la Calle-Mustienes E and Gomez-Skarmeta JL (2013) The developmental epigenomics toolbox: ChIP-seq and MethylCap-seq profiling of early zebrafish embryos. *Methods* **62**(3): 207-215.

Carney SA, Prasch AL, Heideman W and Peterson RE (2006) Understanding dioxin developmental toxicity using the zebrafish model. *Birth Defects Res A Clin Mol Teratol* **76**(1): 7-18.

Chen S, Tao J, Bae Y, Jiang MM, Bertin T, Chen Y, Yang T and Lee B (2013) Notch gain of function inhibits chondrocyte differentiation via Rbpj-dependent suppression of Sox9. *J Bone Miner Res* **28**(3): 649-659.

Chiang EF, Pai CI, Wyatt M, Yan YL, Postlethwait J and Chung B (2001) Two sox9 genes on duplicated zebrafish chromosomes: expression of similar transcription activators in distinct sites. *Dev Biol* **231**(1): 149-163.

Deigan KE, Li TW, Mathews DH and Weeks KM (2009) Accurate SHAPE-directed RNA structure determination. *Proc Natl Acad Sci U S A* **106**(1): 97-102.

Dooley K and Zon LI (2000) Zebrafish: a model system for the study of human disease. *Curr Opin Genet Dev* **10**(3): 252-256.

Esain V, Postlethwait JH, Charnay P and Ghislain J (2010) FGF-receptor signalling controls neural cell diversity in the zebrafish hindbrain by regulating olig2 and sox9. *Development* **137**(1): 33-42.

Fatica A and Bozzoni I (2014) Long non-coding RNAs: new players in cell differentiation and development. *Nat Rev Genet* **15**(1): 7-21.

Furuyama K, Kawaguchi Y, Akiyama H, Horiguchi M, Kodama S, Kuhara T, Hosokawa S, Elbahrawy A, Soeda T, Koizumi M, Masui T, Kawaguchi M, Takaori K, Doi R, Nishi E, Kakinoki R, Deng JM, Behringer RR, Nakamura T and Uemoto S (2011) Continuous cell supply from a Sox9-expressing progenitor zone in adult liver, exocrine pancreas and intestine. *Nat Genet* **43**(1): 34-41.

Garcia GR, Noyes PD and Tanguay RL (2016) Advancements in zebrafish applications for 21st century toxicology. *Pharmacol Ther* **161**: 11-21.

Goodale BC, La Du J, Tilton SC, Sullivan CM, Bisson WH, Waters KM and Tanguay RL (2015) Ligand-Specific Transcriptional Mechanisms Underlie Aryl Hydrocarbon Receptor-Mediated Developmental Toxicity of Oxygenated PAHs. *Toxicol Sci* **147**(2): 397-411.

Goodale BC, La Du JK, Bisson WH, Janszen DB, Waters KM and Tanguay RL (2012) AHR2 mutant reveals functional diversity of aryl hydrocarbon receptors in zebrafish. *PLoS One* **7**(1): e29346.

Gutschner T and Diederichs S (2012) The hallmarks of cancer: a long non-coding RNA point of view. *RNA Biol* **9**(6): 703-719.

Hahn ME, Karchner SI, Shapiro MA and Perera SA (1997) Molecular evolution of two vertebrate aryl hydrocarbon (dioxin) receptors (AHR1 and AHR2) and the PAS family. *Proc Natl Acad Sci U S A* **94**(25): 13743-13748.

Haldin CE and LaBonne C (2010) SoxE factors as multifunctional neural crest regulatory factors. *Int J Biochem Cell Biol* **42**(3): 441-444.

Hao N and Whitelaw ML (2013) The emerging roles of AhR in physiology and immunity. *Biochem Pharmacol* **86**(5): 561-570.

Henry TR, Spitsbergen JM, Hornung MW, Abnet CC and Peterson RE (1997) Early life stage toxicity of 2,3,7,8-tetrachlorodibenzo-p-dioxin in zebrafish (Danio rerio). *Toxicol Appl Pharmacol* **142**(1): 56-68.

Hofsteen P, Plavicki J, Johnson SD, Peterson RE and Heideman W (2013) Sox9b is required for epicardium formation and plays a role in TCDD-induced heart malformation in zebrafish. *Mol Pharmacol* **84**(3): 353-360.

Howe K, Clark MD, Torroja CF, Torrance J, Berthelot C, Muffato M, Collins JE, Humphray S, McLaren K, Matthews L, McLaren S, Sealy I, Caccamo M, Churcher C, Scott C, Barrett JC, Koch R, Rauch GJ, White S, Chow W, Kilian B, Quintais LT, Guerra-Assuncao JA, Zhou Y, Gu Y, Yen J, Vogel JH, Eyre T, Redmond S, Banerjee R, Chi J, Fu B, Langley E, Maguire SF, Laird GK, Lloyd D, Kenyon E, Donaldson S, Sehra H, Almeida-King J, Loveland J, Trevanion S, Jones M, Quail M, Willey D, Hunt A, Burton J, Sims S, McLay K, Plumb B, Davis J, Clee C, Oliver K, Clark R, Riddle C, Elliot D, Threadgold G, Harden G, Ware D, Begum S, Mortimore B, Kerry G, Heath P, Phillimore B, Tracey A, Corby N, Dunn M, Johnson C, Wood J, Clark S, Pelan S, Griffiths G, Smith M, Glithero R, Howden P, Barker N, Lloyd C, Stevens C, Harley J, Holt K, Panagiotidis G, Lovell J, Beasley H, Henderson C, Gordon D, Auger K, Wright D, Collins J, Raisen C, Dyer L, Leung K, Robertson L, Ambridge K, Leongamornlert D, McGuire S, Gilderthorp R, Griffiths C, Manthravadi D, Nichol S, Barker G, Whitehead S, Kay M, Brown J, Murnane C, Gray E, Humphries M, Sycamore N, Barker D,

Saunders D, Wallis J, Babbage A, Hammond S, Mashreghi-Mohammadi M, Barr L, Martin S, Wray P, Ellington A, Matthews N, Ellwood M, Woodmansey R, Clark G, Cooper J, Tromans A, Grafham D, Skuce C, Pandian R, Andrews R, Harrison E, Kimberley A, Garnett J, Fosker N, Hall R, Garner P, Kelly D, Bird C, Palmer S, Gehring I, Berger A, Dooley CM, Ersan-Urun Z, Eser C, Geiger H, Geisler M, Karotki L, Kirn A, Konantz J, Konantz M, Oberlander M, Rudolph-Geiger S, Teucke M, Lanz C, Raddatz G, Osoegawa K, Zhu B, Rapp A, Widaa S, Langford C, Yang F, Schuster SC, Carter NP, Harrow J, Ning Z, Herrero J, Searle SM, Enright A, Geisler R, Plasterk RH, Lee C, Westerfield M, de Jong PJ, Zon LI, Postlethwait JH, Nusslein-Volhard C, Hubbard TJ, Roest Crollius H, Rogers J and Stemple DL (2013) The zebrafish reference genome sequence and its relationship to the human genome. *Nature* **496**(7446): 498-503.

Huang B, Wang S, Ning Y, Lamb AN and Bartley J (1999) Autosomal XX sex reversal caused by duplication of SOX9. *Am J Med Genet* **87**(4): 349-353.

Huang S, Shui X, He Y, Xue Y, Li J, Li G, Lei W and Chen C (2015) AhR expression and polymorphisms are associated with risk of coronary arterial disease in Chinese population. *Sci Rep* **5**: 8022.

Jo A, Denduluri S, Zhang B, Wang Z, Yin L, Yan Z, Kang R, Shi LL, Mok J, Lee MJ and Haydon RC (2014) The versatile functions of Sox9 in development, stem cells, and human diseases. *Genes Dis* **1**(2): 149-161.

Karabiber F, McGinnis JL, Favorov OV and Weeks KM (2013) QuShape: rapid, accurate, and best-practices quantification of nucleic acid probing information, resolved by capillary electrophoresis. *RNA* **19**(1): 63-73.

Kaushik K, Leonard VE, Kv S, Lalwani MK, Jalali S, Patowary A, Joshi A, Scaria V and Sivasubbu S (2013) Dynamic expression of long non-coding RNAs (lncRNAs) in adult zebrafish. *PLoS One* **8**(12): e83616.

Kettleborough RN, Busch-Nentwich EM, Harvey SA, Dooley CM, de Bruijn E, van Eeden F, Sealy I, White RJ, Herd C, Nijman IJ, Fenyes F, Mehroke S, Scahill C, Gibbons R, Wali N, Carruthers S, Hall A, Yen J, Cuppen E and Stemple DL (2013) A systematic genome-wide analysis of zebrafish protein-coding gene function. *Nature* **496**(7446): 494-497.

Kim H, Cordero P, Das R and Yoon S (2013) HiTRACE-Web: an online tool for robust analysis of high-throughput capillary electrophoresis. *Nucleic Acids Res* **41**(Web Server issue): W492-498.

Kladwang W, VanLang CC, Cordero P and Das R (2011) A two-dimensional mutate-and-map strategy for non-coding RNA structure. *Nature chemistry* **3**(12): 954-962.

Kleindienst A, Dunbar JG, Glisson R, Okuno K and Marmarou A (2006) Effect of dimethyl sulfoxide on blood-brain barrier integrity following middle cerebral artery occlusion in the rat. *Acta Neurochir Suppl* **96**: 258-262.

Knecht AL, Goodale BC, Truong L, Simonich MT, Swanson AJ, Matzke MM, Anderson KA, Waters KM and Tanguay RL (2013) Comparative developmental toxicity of environmentally relevant oxygenated PAHs. *Toxicol Appl Pharmacol* **271**(2): 266-275.

Knecht AL, Truong L, Simonich MT and *Tanguay RL (2016) Developmental benzo[a]pyrene (B[a]P) exposure impacts larval behavior and impairs adult learning in zebrafish. *Neurotoxicology and teratology*.

Kohn A, Rutkowski TP, Liu Z, Mirando AJ, Zuscik MJ, O'Keefe RJ and Hilton MJ (2015) Notch signaling controls chondrocyte hypertrophy via indirect regulation of Sox9. *Bone Res* **3**: 15021.

Livak KJ and Schmittgen TD (2001) Analysis of relative gene expression data using real-time quantitative PCR and the 2(-Delta Delta C(T)) Method. *Methods* **25**(4): 402-408.

Lorenz R, Bernhart SH, Honer Zu Siederdissen C, Tafer H, Flamm C, Stadler PF and Hofacker IL (2011) ViennaRNA Package 2.0. *Algorithms Mol Biol* **6**: 26.

Martini S, Bernoth K, Main H, Ortega GD, Lendahl U, Just U and Schwanbeck R (2013) A critical role for Sox9 in notch-induced astrogliogenesis and stem cell maintenance. *Stem Cells* **31**(4): 741-751.

Matheu A, Collado M, Wise C, Manterola L, Cekaite L, Tye AJ, Canamero M, Bujanda L, Schedl A, Cheah KS, Skotheim RI, Lothe RA, Lopez de Munain A, Briscoe J, Serrano M and Lovell-Badge R (2012) Oncogenicity of the developmental transcription factor Sox9. *Cancer Res* **72**(5): 1301-1315.

Mercer TR, Dinger ME, Sunkin SM, Mehler MF and Mattick JS (2008) Specific expression of long noncoding RNAs in the mouse brain. *Proc Natl Acad Sci U S A* **105**(2): 716-721.

Ohba S, He X, Hojo H and McMahon AP (2015) Distinct Transcriptional Programs Underlie Sox9 Regulation of the Mammalian Chondrocyte. *Cell Rep* **12**(2): 229-243.

Pardridge WM (2005) The blood-brain barrier: bottleneck in brain drug development. *NeuroRx* **2**(1): 3-14.

Plavicki JS, Baker TR, Burns FR, Xiong KM, Gooding AJ, Hofsteen P, Peterson RE and Heideman W (2014) Construction and characterization of a sox9b transgenic reporter line. *Int J Dev Biol* **58**(9): 693-699.

Postlethwait J, Amores A, Cresko W, Singer A and Yan YL (2004) Subfunction partitioning, the teleost radiation and the annotation of the human genome. *Trends Genet* **20**(10): 481-490.

Prasch AL, Tanguay RL, Mehta V, Heideman W and Peterson RE (2006) Identification of zebrafish ARNT1 homologs: 2,3,7,8-tetrachlorodibenzo-p-dioxin toxicity in the developing zebrafish requires ARNT1. *Mol Pharmacol* **69**(3): 776-787.

Pritchett J, Athwal V, Roberts N, Hanley NA and Hanley KP (2011) Understanding the role of SOX9 in acquired diseases: lessons from development. *Trends Mol Med* **17**(3): 166-174.

Quinn JJ and Chang HY (2016) Unique features of long non-coding RNA biogenesis and function. *Nat Rev Genet* **17**(1): 47-62.

Schneider AJ, Branam AM and Peterson RE (2014) Intersection of AHR and Wnt signaling in development, health, and disease. *Int J Mol Sci* **15**(10): 17852-17885.

Scott CE, Wynn SL, Sesay A, Cruz C, Cheung M, Gomez Gaviro MV, Booth S, Gao B, Cheah KS, Lovell-Badge R and Briscoe J (2010) SOX9 induces and maintains neural stem cells. *Nat Neurosci* **13**(10): 1181-1189.

Simon MD (2013) Capture hybridization analysis of RNA targets (CHART). *Curr Protoc Mol Biol* **Chapter 21**: Unit 21 25.

Spitsbergen JM and Kent ML (2003) The State of the Art of the Zebrafish Model for Toxicology and Toxicologic Pathology Research-Advantages and Current Limitations. *Toxicol Pathol* **31 Suppl**: 62-87.

Stolt CC and Wegner M (2010) SoxE function in vertebrate nervous system development. *Int J Biochem Cell Biol* **42**(3): 437-440.

Thisse C and Thisse B (2008) High-resolution in situ hybridization to whole-mount zebrafish embryos. *Nat Protocols* **3**(1): 59-69.

Truong L, Harper SL and Tanguay RL (2011) Evaluation of Embryotoxicity Using the Zebrafish Model, in *Drug Safety Evaluation: Methods and Protocols* (Gautier J-C ed) pp 271-279, Humana Press, Totowa, NJ.

Turner DH and Mathews DH (2010) NNDB: the nearest neighbor parameter database for predicting stability of nucleic acid secondary structure. *Nucleic Acids Res* **38**(Database issue): D280-282.

Vasa SM, Guex N, Wilkinson KA, Weeks KM and Giddings MC (2008) ShapeFinder: a software system for high-throughput quantitative analysis of nucleic acid reactivity information resolved by capillary electrophoresis. *RNA* **14**(10): 1979-1990.

Vezina CM, Lin TM and Peterson RE (2009) AHR signaling in prostate growth, morphogenesis, and disease. *Biochem Pharmacol* **77**(4): 566-576.

Wall RJ, Fernandes A, Rose M, Bell DR and Mellor IR (2015) Characterisation of chlorinated, brominated and mixed halogenated dioxins, furans and biphenyls as potent and as partial agonists of the Aryl hydrocarbon receptor. *Environ Int* **76**: 49-56.

Westerfield M (2007) *The Zebrafish Book. A Guide for the Laboratory Use of Zebrafish (Danio rerio)*. 5th ed. University of Oregon Press, Eugene, Oregon.

Xiong KM, Peterson RE and Heideman W (2008) Aryl hydrocarbon receptor-mediated down-regulation of sox9b causes jaw malformation in zebrafish embryos. *Mol Pharmacol* **74**(6): 1544-1553.

Yan YL, Willoughby J, Liu D, Crump JG, Wilson C, Miller CT, Singer A, Kimmel C, Westerfield M and Postlethwait JH (2005) A pair of Sox: distinct and overlapping functions of zebrafish sox9 co-orthologs in craniofacial and pectoral fin development. *Development* **132**(5): 1069-1083.

Zhu MY, Gasperowicz M and Chow RL (2013) The expression of NOTCH2, HES1 and SOX9 during mouse retinal development. *Gene Expr Patterns* **13**(3-4): 78-83.

**FOOTNOTES**

This research was partially supported by National Institutes of Health grants [P42 ES016465], [R21 ES025421], [T32 ES07060], [F31 ES026518], [F32 ES025082], and [P30 ES000210]. The content is solely the responsibility of the authors and does not necessarily represent the official views of the National Institutes of Health.

Molecular Pharmacology Fast Forward. Published on April 6, 2017 as DOI: 10.1124/mol.117.108233
This article has not been copyedited and formatted. The final version may differ from this version.



## FIGURE LEGENDS

**Figure 1 The *slincR* and *sox9b* locus on chromosome 3, subcellular enrichment, and SHAPE enhanced prediction of *slincR* secondary structure.** (A), Schematic diagram of the *slincR* and *sox9b* locus on chromosome 3 (not to scale). The Ensembl splice variant *si:Ch1073-384e4.1* is not depicted for clarity. (B), Subcellular enrichment of *slincR* in 96 hpf whole embryos. qRT-PCR was performed on whole embryo, cytoplasmic, and nuclear homogenate samples. *U1* rRNA served as a positive control for nuclear enrichment. Expression values were analyzed with the $2^{-\Delta\Delta CT}$ method; however, we did not normalize to a reference gene. Results for (B) were statistically analyzed using a paired *t*-test and corrected for multiple comparisons using the Holm-Sidak method, with $\alpha = 0.05$. Error bars indicate SD of the mean. *** = $p < 0.001$ compared to whole embryo. (C) *SlincR*'s predicted secondary structure. Selective 2′-hydroxyl acylation analyzed by primer extension (SHAPE) was run in triplicate from 3 independent samples. We normalized the data to be between 0 and 2 and entered the SHAPE reactivities into RNAfold. Unreactive nucleotides (white) participate in canonical base pairs; whereas, nucleotides in loops, bulges, and other connecting regions are reactive (blue)

**Figure 2 *SlincR* and *sox9b*-eGFP are expressed in adjacent and overlapping tissues through multiple stages of development.** Lateral (A) and ventral (B) view of dual immunohistochemistry and *in situ* hybridization samples targeting *sox9b*-eGFP (green) and *slincR* (red) in *sox9b*-eGFP reporter fish at 36 and 48 hpf ($n$ = 6-10 embryos). The fish are outlined with a white line, *slincR* expression is outlined with a dotted white line, and the eye is labeled with 'e'. The white rectangle represents the magnified area depicted in the inset. Both scale bars represent 100 μm. All experiments were independently repeated a minimum of 2 times.

**Figure 3 Comparative analysis of AHR2 functional status and *slincR* expression levels and spatial pattern relative to *sox9b*.** (A) *SlincR* expression in 48 hpf wild type 5D ($AHR2^{+/+}$) and AHR2-null ($AHR2^{-/-}$) whole embryos developmentally exposed to 0.1% DMSO (vehicle control) or

Molecular Pharmacology Fast Forward. Published on April 6, 2017 as DOI: 10.1124/mol.117.108233
This article has not been copyedited and formatted. The final version may differ from this version.



1 ng/mL TCDD (*n* = 3 biological replications). Results were statistically analyzed using GraphPad Prism 7.02 software. The data was tested for normality using the Shapiro-Wilk normality test, analyzed with a two-way ANOVA, and a correction for multiple comparisons was performed using the Dunnett's test (95% confidence intervals). Error bars indicate SD of the mean. ** = $p < 0.01$ compared to DMSO control. ǂ ǂ = $p < 0.01$ compared to TCDD control. (B) Dorsal view of dual immunohistochemistry and *in situ* hybridization samples targeting *sox9b*-eGFP (green) and *slincR* (red) in 48 hpf embryos (*n* = 6-10 embryos). The *Tg*(*−2421/+29sox9b:EGFP*$_{uw2}$) *sox9b* reporter line embryos were developmentally exposed to 0.1% DMSO or 1 ng/mL TCDD. In the TCDD-exposed samples, the regions with increased *slincR* expression had a corresponding decrease in *sox9b*-eGFP expression (white rectangle). e = eye, ov = otic vesicle, p = pectoral fin, fb = forebrain, mb = midbrain, and hb = hindbrain. 100 μm scale bar. All experiments were independently repeated a minimum of 2 times.

**Figure 4 Comparative analysis of the relative expression of *slincR* and *sox9 in TCDD-exposed samples.*** *SlincR* (A) and *sox9b* mRNA (B) quantitative expression in 48 hpf whole embryo *slincR* (*slincR*-MO) and control (ConMO) morphants developmentally exposed to 0.1% DMSO (vehicle control) or 1 ng/mL TCDD. For all qPCR data, expression values were analyzed with the $2^{-\Delta\Delta CT}$ method. Expression values were normalized to β-*actin* and the control morphants served as the calibrator. Samples represent a minimum of 3 biological replicates. Results were statistically analyzed using GraphPad Prism 7.02 software. The data was tested for normality using the Shapiro-Wilk normality test and analyzed with a two-way ANOVA and a correction for multiple comparisons was performed using the Dunnett's test (95% confidence intervals). Error bars indicate SD of the mean. * = $p < 0.05$, ** = $p < 0.01$ compared to controls. ǂ ǂ = $p < 0.01$ compared to TCDD control. (C-F) dorsal and lateral views of *in situ* hybridization samples targeting *slincR* (red) and *sox9b* (blue) in 48 hpf (C, E, F) and 72 hpf (D) embryos (*n* = 6-10 embryos). (C-D) Are representative images from control morphants. In the TCDD-exposed

Molecular Pharmacology Fast Forward. Published on April 6, 2017 as DOI: 10.1124/mol.117.108233
This article has not been copyedited and formatted. The final version may differ from this version.



samples, *slincR* morphants displayed increased *sox9b* expression patterns compared to controls (white rectangle, which represents the magnified image in the inset). The fish are outlined with a white line. e = eye, ov = otic vesicle, p = pectoral fin, and mb = midbrain. 100 μm scale bar. All experiments were independently repeated a minimum of 2 times.

**Figure 5 Comparative analysis of the relative expression of *sox9b* and downstream targets in *slincR* morphants.** (A) Quantitative expression levels of *sox9b* and downstream targets in *slincR* and control morphants at 48 hpf. Five out of the 9 downstream target genes were significantly different when compared to control morphants. Expression values were analyzed with the $2^{-\Delta\Delta CT}$ method, normalized to β-*actin,* and the control morphants served as the calibrator. Samples represent a minimum of 3 biological replicates. Results were statistically analyzed using GraphPad Prism 7.02 software. The data was tested for normality using the Shapiro-Wilk normality test, analyzed using a paired *t*-test, and corrected for multiple comparison using the Holm-Sidak method, with alpha = 0.05. Error bars indicate SD of the mean, * = $p < 0.05$, ** = $p < 0.01$ compared to controls. Dorsal, ventral, and lateral views of *in situ* hybridization samples targeting *notch3* (B) and *adamts3* (C) in 48 hpf *slincR* and control morphants ($n$ = 6-10 embryos). e = eye, ov = otic vesicle, p = pectoral fin, s = somite, and mb = midbrain. 100 μm scale bar.

**Figure 6 Phenotypic analysis of a reduction in *slincR* expression during early development.** (A), An 18-endpoint morphological screen in *slincR* and control morphants at 120 hpf ($n$ = 24). No significant malformations were observed in the *slincR* morphants. Control and *slincR* morphants evaluations were completed in a binary notation (present/absent) and statistically compared using Fisher's exact test at $p < 0.05$ for each endpoint. (B) Larval photomotor response (LPR) in control and *slincR* morphants at 120 hpf ($n$ = 23) using the Viewpoint Zebrabox systems. *SlincR* morphants displayed a hypoactive response ($p < 0.01$), with a -14.04% difference of the mean area under the curve when compared to controls. The LPR assay consisted of 3 minutes of light and dark alternating periods, for a total of four light-dark

transitions, with the first transition representing an acclimation period. The black and white bar along the y-axis indicates the 3 minutes of light (white) and dark (black) alternating periods. Larval zebrafish at this developmental stage display increased locomotion during periods of darkness. The overall area under the curve was analyzed for the last 3 light-dark cycles compared to control morphants using a Kolmogorov-Smirnov test ($p < 0.01$). All experiments were independently repeated a minimum of 2 times.

Molecular Pharmacology Fast Forward. Published on April 6, 2017 as DOI: 10.1124/mol.117.108233
This article has not been copyedited and formatted. The final version may differ from this version.



## TABLES

Table 1 *slincR* expression at multiple developmental stages

| *slincR* expression | 24 hpf | 36 hpf | 48 hpf | 60 hpf | 72 hpf |
|---|---|---|---|---|---|
| Heart | N | N | N | N | N |
| Brain | N | N | N | N | N |
| Otic Vesicle | N | Y | Y | Y | Y |
| Eye | N | Y | Y | Y | Y |
| Jaw/Snout | N | Y | Y | Y | Y |
| Pectoral Bud/Fin | N | N | N | N | N |
| Notochord | N | N | N | N | N |

*Note: 6-10 embryos were scored at each time point for each organ or structure*

*N = No; Y = Yes*

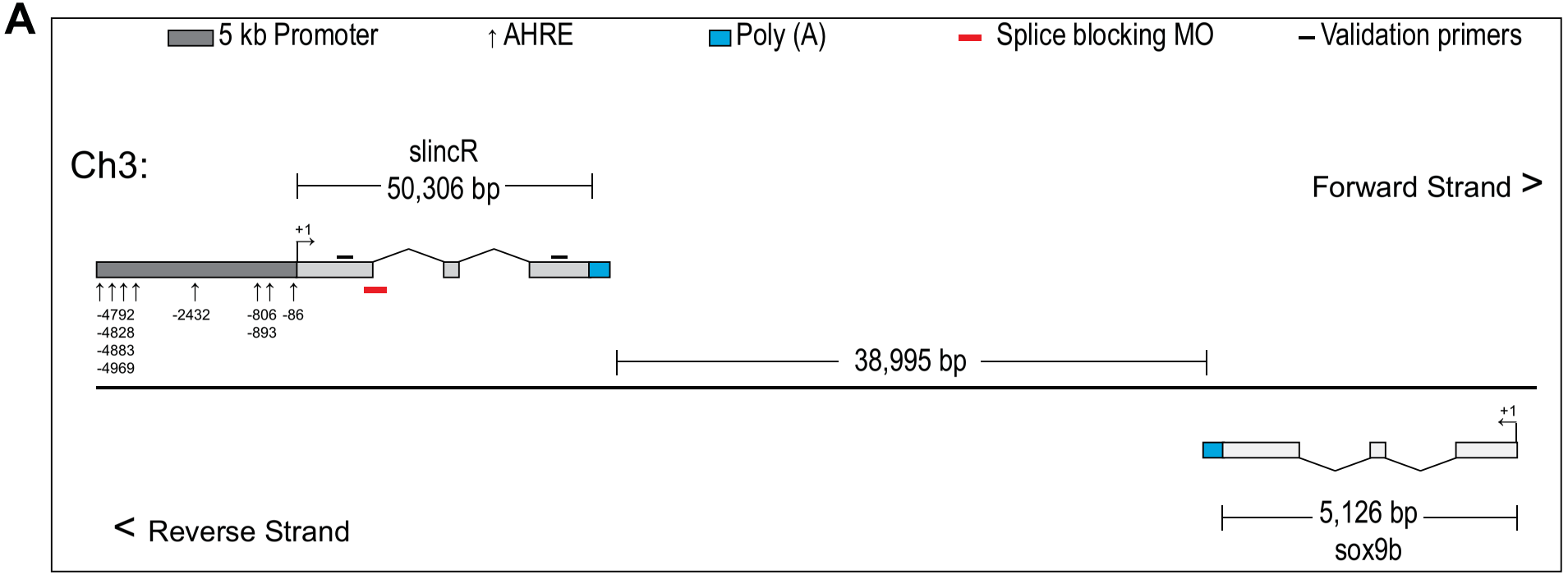


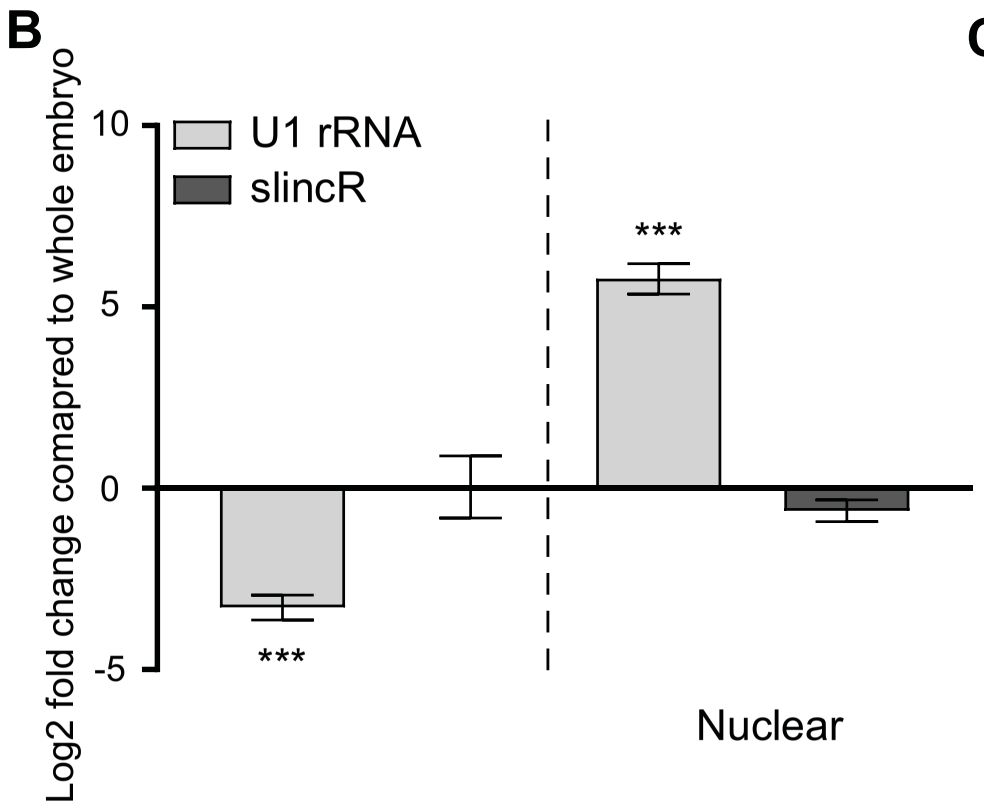


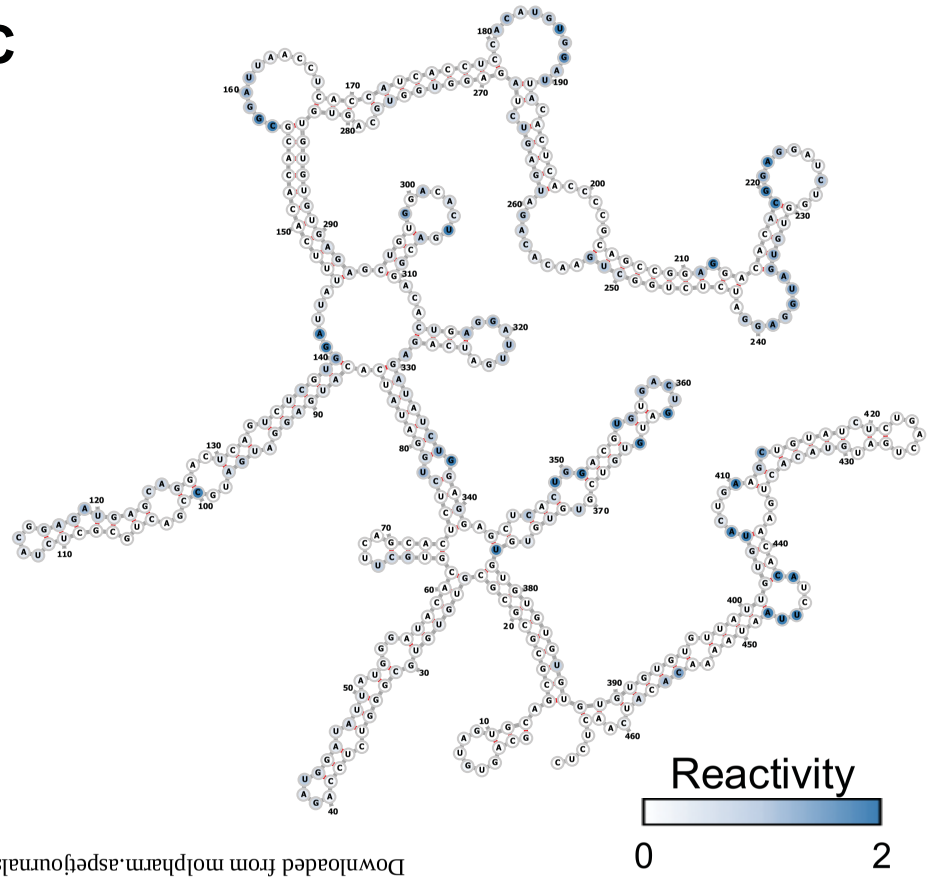


Figure 1

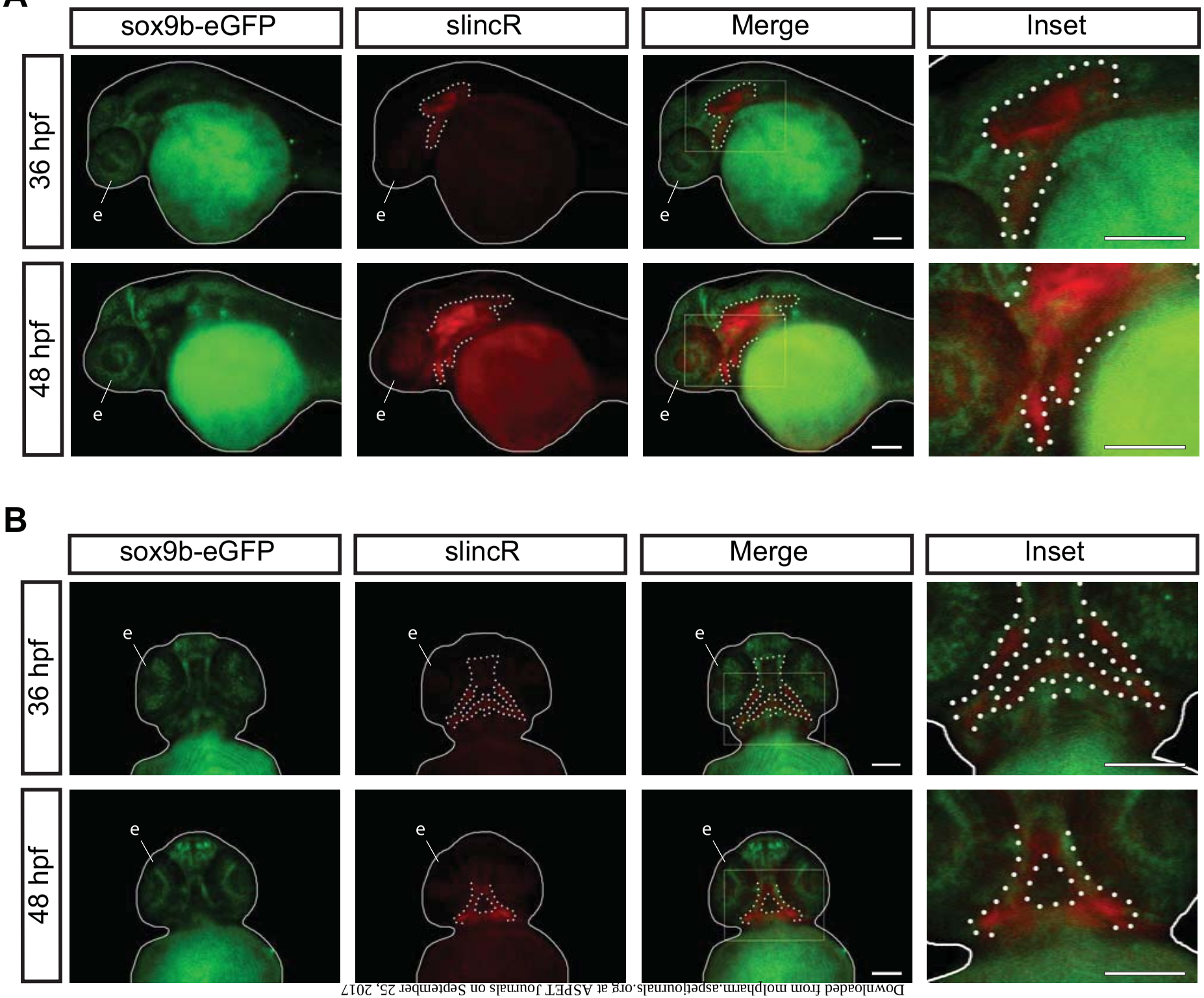

Figure 3

Molecular Pharmacology Fast Forward. Published on April 6, 2017 as DOI: 10.1124/mol.117.108233
This article has not been copyedited and formatted. The final version may differ from this version.

Figure 4

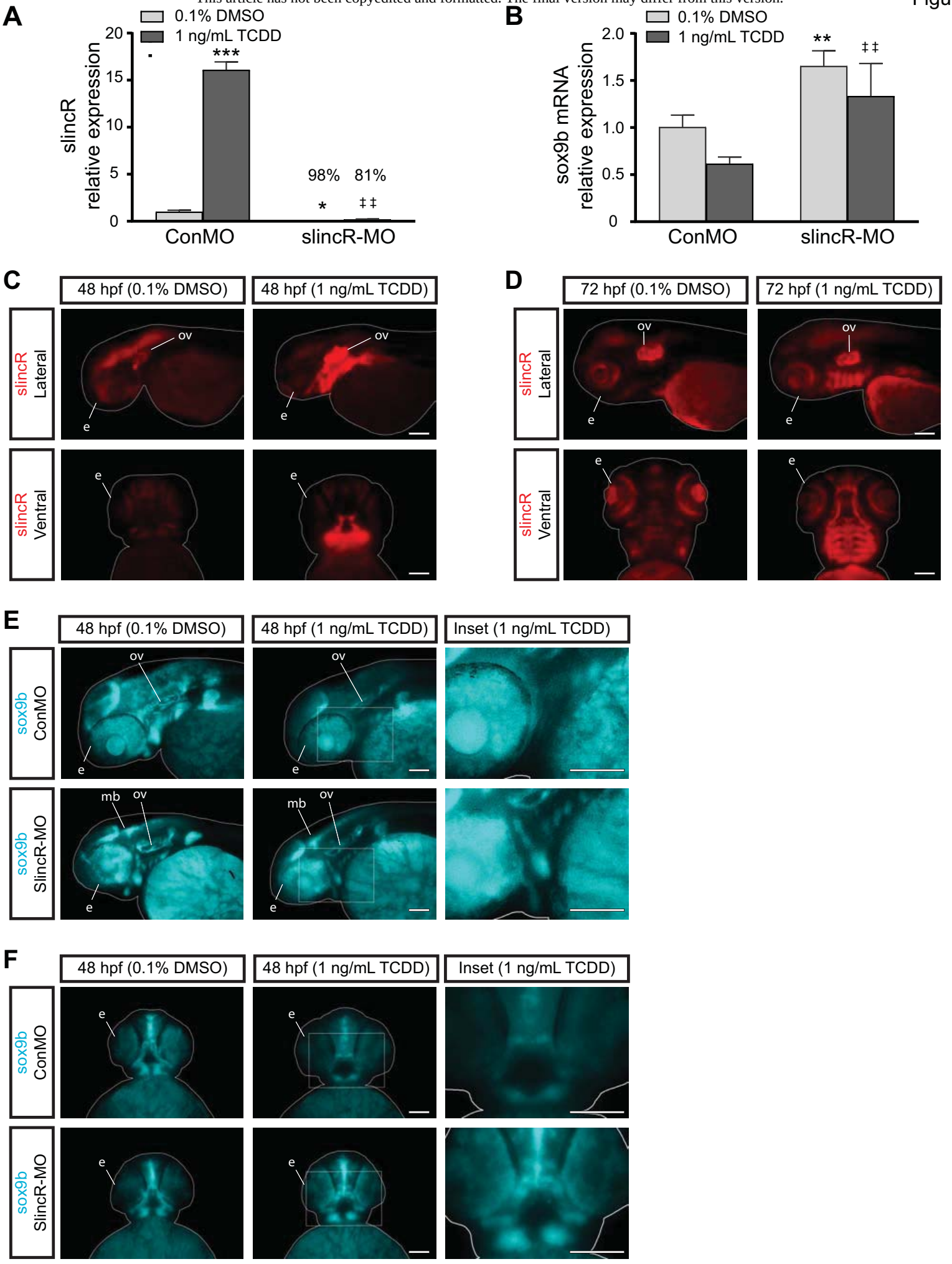

Molecular Pharmacology Fast Forward. Published on April 6, 2017 as DOI: 10.1124/mol.117.108233
This article has not been copyedited and formatted. The final version may differ from this version.

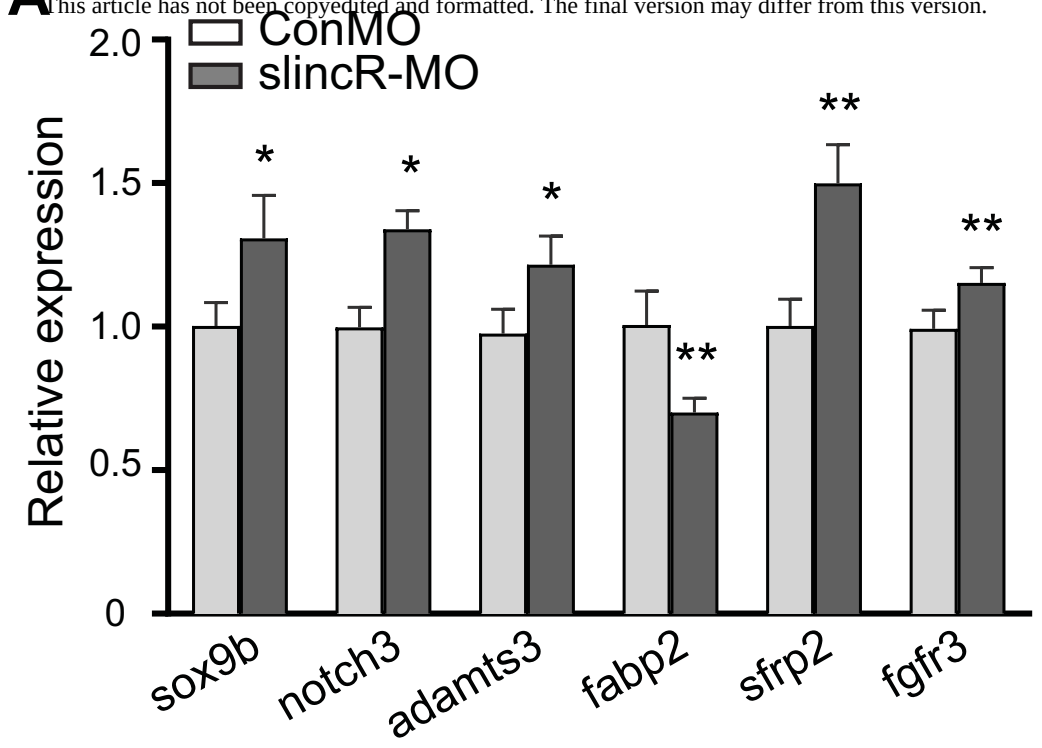


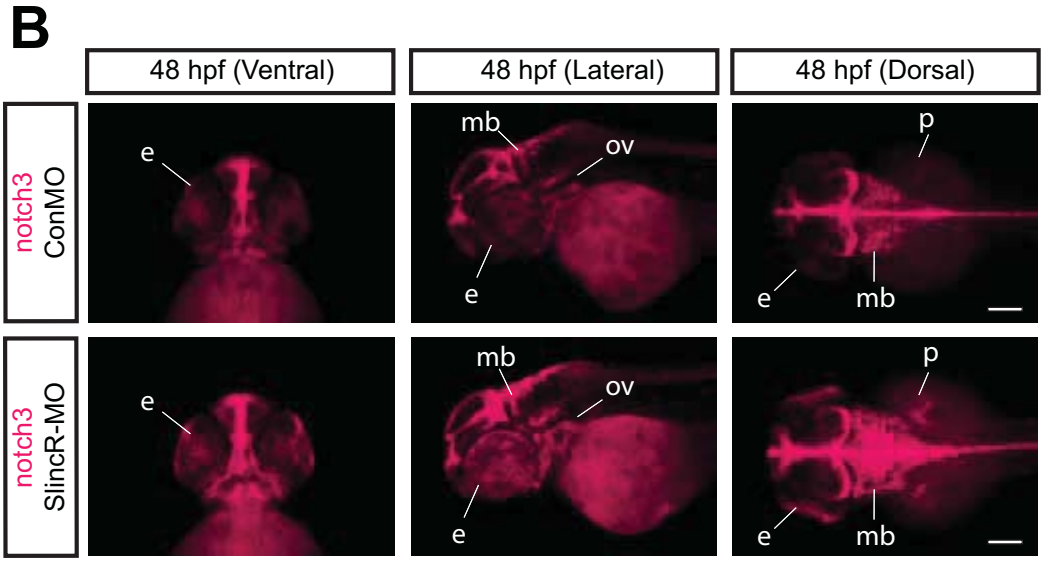


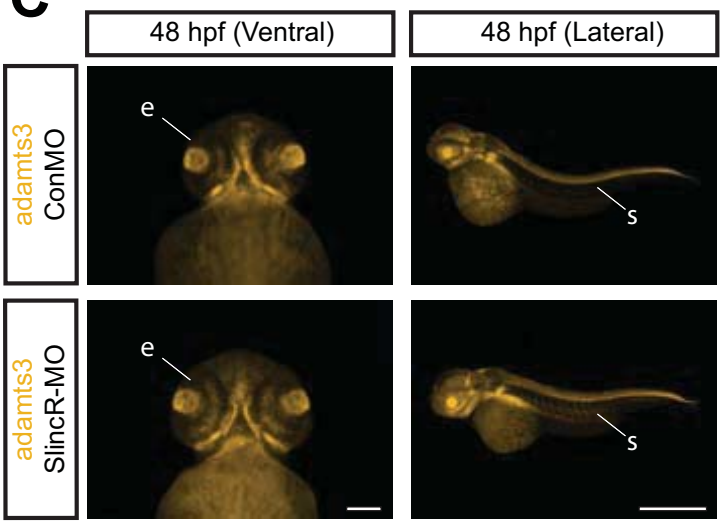


Figure 5

Molecular Pharmacology Fast Forward. Published on April 6, 2017 as DOI: 10.1124/mol.117.108233
This article has not been copyedited and formatted. The final version may differ from this version.

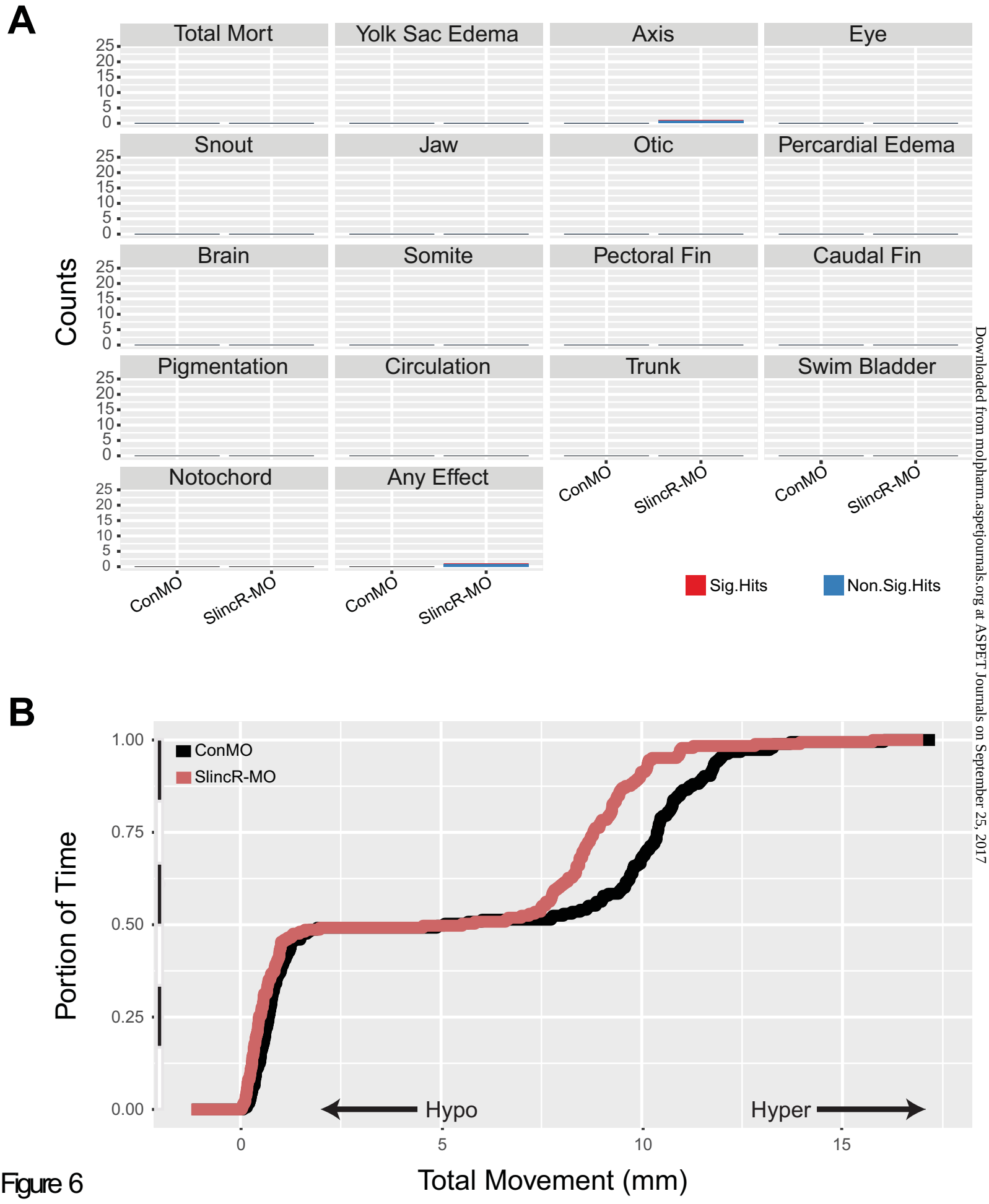


Figure 6